JOURNAL OF PROPULSION AND POWER
Vol. 21, No. 4, July–August 2005

Role of Injection in Hybrid Rockets Regression Rate Behavior

Carmine Carmicino* and Annamaria Russo Sorge†
University of Naples "Federico II," 80125 Naples, Italy

A series of firing tests was carried out to investigate the influence of the oxidizer injection on the solid fuel regression rate behavior in a hybrid rocket engine. For this purpose, a conical subsonic nozzle as the injector of the gaseous oxidizer was selected to generate nonuniform conditions at the entrance of the fuel port. Gaseous oxygen and polyethylene fuel cylindrical grains were used. When the oxygen was fed by this kind of injector, the fuel regression in the region of the oxygen impingement on the grain's surface was increased several times, which led to irregular fuel consumption with the characteristic afterburn port shape typical of solid fuel ramjets having a rearward-facing step at the air inlet. The local instantaneous regression rates, measured by means of the ultrasound pulse-echo technique, showed regression rate-time profiles strongly dependent on the geometric configuration and helped to explain the complex regression phenomenon deriving from the impingement zone displacement during the time. Empirical correlations for the prediction of the average regression rate were developed taking into account the influence of mass flux, pressure, and port diameter. Finally, a nondimensional semi-empirical correlation involving the effect of the blowing number yielded improved accuracy.

Nomenclature

A	=	preexponential factor, mm/s
B	=	blowing number
c_{ref}	=	speed of ultrasounds in reference conditions, m/s
D	=	port diameter, mm
D_e	=	grain outer diameter, mm
d	=	injector exit diameter, mm
E_a	=	activation energy, kcal/mole
G	=	total mass flux, kg/m^{2}s
H_v	=	effective heat of vaporization, J/kg
L	=	grain length, mm
L_c	=	prechamber length, mm
M	=	solid fuel mass, kg
$\dot{m}$	=	mass flow rate, kg/s
Nu	=	Nusselt number based on port diameter
O/F	=	average oxidizer to fuel ratio
Pr	=	Prandtl number
p	=	pressure, atm
Re_D	=	Reynolds number based on port diameter
R_g	=	gas constant, 1.986 cal/mole K
R^2	=	squared correlation factor
$\dot{r}$	=	regression rate, mm/s
St	=	Stanton number
s	=	fuel grain thickness, mm
T_w	=	fuel surface temperature, K
t	=	time, s
x	=	axial abscissa, mm
$x_{\max}$	=	abscissa of maximum fuel consumption point, mm
Δt	=	burn time, s
ρ_f	=	solid fuel density, kg/m^3

Subscripts

e	=	grain external surface
j	=	injector effect
ox	=	oxidizer
0	=	initial
2	=	final

Superscript

$-$	=	average value

Introduction

THE hybrid rocket motor is known to provide several distinct advantages over both solid-propellant and liquid-propellant motors. Simplicity, safety, lower cost, and thrust tailoring are among the hybrid's most attractive features.

The solid fuel regression rate represents the key parameter for a thorough characterization of the hybrid internal ballistics; thus, a deep knowledge of the regression physical process is compulsory to assist in the motor design.

It was widely demonstrated, in both theoretical and experimental works, only some of which are cited here,[1–4] that, at the motor operating conditions, in the absence of radiation, the regression rate mostly depends on the convective heat transfer from the flame to the fuel surface. Marxman and Gilbert[1] and Marxman[2] developed a turbulent boundary-layer regression rate model yielding the important result that, in this regime, the mass flux is the fundamental factor governing the rate of fuel consumption ($\dot{r} \propto G^{0.8}$). Furthermore, the regression rate is a weak function of the axial distance ($\dot{r} \propto x^{-0.2}$), as well as of propellant properties ($\dot{r} \propto B^{0.23}$).

Pressure was also found to influence the regression rate for certain fuels and regimes of operation (principally at lower and higher mass fluxes) by several investigators who, on achieving high mass fluxes, attributed this effect to either the wall heterogeneous reactions with the oxidizer[5] or the finite rate gas-phase chemical kinetics.[6] Another reason why a pressure-dependent regression rate can be observed is radiation. The radiative heat transfer to the solid fuel surface is strongly affected by pressure, and its relative contribution to the total heat transfer can become significant at low values of the total mass flux and if the combustion products contain a high concentration of particles.[7]

Moreover, the oxidizer injection characteristics have significant weight because the whole combustion process will be severely affected by the incoming oxidizer flow pattern. A geometrical effect that is important but very difficult to assess is represented by the oxidizer entrance conditions. Although the latter may be conceived as determining second order effects in classical hybrid systems, as this is also mentioned in Ref. 8, our tests showed that they are critical. Actually, if the oxidizer is fed into the port by an axial

Received 8 April 2004; revision received 23 November 2004; accepted for publication 14 January 2005.

*Postdoctoral Appointee, Department of Space Science and Engineering, Piazzale L. G. Napolitano, Tecchio 80. Member AIAA.

†Associate Professor, Department of Space Science and Engineering, Piazzale L. G. Napolitano, Tecchio 80. Member AIAA.

nozzle, the convective heat flux in the recirculation and the subsequent impingement regions is completely different from the one in the fully developed turbulent flow, and the resulting regression rates are both increased and unevenly distributed along the axis. This feature substantially concerns all grain length to initial diameter ratios tested here because, as the fuel regresses, its port diameter increases, and the oxidizer jet tends to impinge on the grain's surface farther downstream, so that the grain portion affected by the impingement becomes wider.

This aspect, of course, has to be carefully examined to minimize the unburned fuel and, at the same time, to try to raise the regression rate for motor applications that do not require the highest thrusts. The increased fuel regression observed near the oxidizer impingement region is not predicted by usual ballistic models; rather, it is in contrast with the results provided in Refs. 1 and 2. Indeed, a fairly uniform axial regression rate attaining a minimum for a certain L/D_0 is predicted by the regression rate equation of Marxman and Gilbert[1] applied to a cylindrical grain because of the combination of the increasing mass flux and the boundary-layer growth down the port. No systematic experimental study has so far been reported on the effect of injector geometry in classical hybrid configurations. Hence, additional research is needed to develop a useful design tool.

The main target of this work was the characterization of the regression rate in the axisymmetric hybrid motor developed at the University of Naples. Overall fuel consumption and local fuel thickness time evolution measurements, the latter performed with the ultrasound pulse-echo technique, were used to this end.

The topics introduced hereafter represent the result of both tests and analysis carried out during two years of work in which the propulsion laboratory was set up. In fact, the major progress over the previous works lies in the number of tests conducted and in the way the data were processed. In particular, in Ref. 9, there were fewer tests, and the grain thickness–time profiles were approximated by analytical functions with the aim of investigating the pressure effect on the regression rate. However, this practice is now believed by the authors to be misleading, whereas the way the regression rate profiles are presented here is certainly more correct. Furthermore, as can be concluded from this paper, a geometrical effect seems predominant in determining the regression rate or, at least, that the pressure influence needs additional examinations. Finally, here the blowing number calculation was performed more exactly, whereas in Ref. 10 it was simply approximated in terms of the mixture ratio.

Experimental Test Facility

A schemematic of the test facility is given in Ref. 11. Gaseous oxygen is fed at mass flow rates up to 0.3 kg/s that are measured with a venturi tube. The oxygen is injected into the chamber through a converging nozzle whose exit diameter is 8 mm. The exit Mach number is at most 0.39. Nitrogen is purged into the chamber by a switch valve (oxygen or nitrogen) for the burnout and in case of an accident. A pyrotechnic igniter was used for the ignition.

The axisymmetric combustion chamber (see Fig. 1), with a 720-mm length and a 133-mm inner case diameter, is designated to operate at pressures up to 40 atm. Cylindrical one-port high-density polyethylene fuel grains, 560 mm long, were tested. Four initial inner diameters, 16, 25, 50, and 75 mm, were used to achieve a wide range of mass fluxes and grain length to diameter ratios. Two chambers were placed before and after the grain the first one to shift toward the fore end of the grain the strong recirculation region caused by the oxygen injection in an attempt to

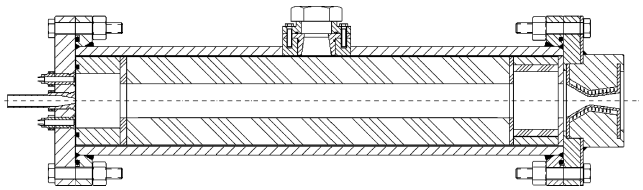

Fig. 1 Hybrid rocket engine scheme.

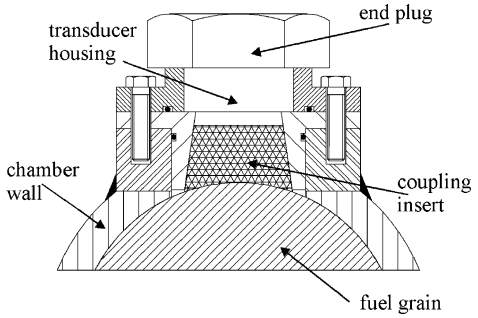

Fig. 2 Ultrasonic transducer–fuel grain coupling.

increase the overall regression rates and the second one to promote the complete gas mixing, thereby improving the combustion efficiency.

A water-cooled De Laval nozzle with a 16-mm throat diameter and an area ratio equal to 2.44, made of copper alloy, ensures long time tests with almost constant pressure. Chamber pressure is measured by two capacitive transducers, Setra model 280E, set up in the prechamber and in the mixing chamber. All of the signals are sampled at 100 Hz, recorded, and processed by software that also controls the system.

The instantaneous regression rate is measured by means of ultrasound equipment. One ultrasonic transducer, located around the middle of the chamber (Fig. 1), is employed to obtain the time evolution of the local grain thickness and, in turn, the regression rate at that point.

The ultrasonic transducer is a Panametrics Videoscan V114-SB of $\frac{3}{4}$ in. nominal diameter and 1 MHz central frequency. It is placed on a coupling insert to better interface the transducer's wear plate with the grain's cylindrical surface (Fig. 2).

A thin layer of glycerine is applied between the wear plate and the insert's top to ensure proper acoustic matching between the surfaces. A silicon gel is applied between the insert and the fuel grain to achieve low acoustic attenuation. The signals emitted by the transducer are generated and amplified by a receiver unit (Panametrics Model 5072PR), are acquired by an oscilloscope, and are processed with an oscilloscope proper function that instantaneously calculates the time lapse between the trigger event (transmitted wave) and the first zero crossing point with a positive slope of the surface echo waveform with a frequency of 10 Hz. This frequency is limited by the oscilloscope performance but, because the fuel may have a regression rate of 1 mm/s or lower, for quasi-steady applications, this seems to be a working value.

Data Reduction

The grain thickness value was calculated with the following formula that holds only if the wave speed is constant[12]:

$$s = c_{\text{ref}} t_0 / 2 \tag{1}$$

where t_0 is the double of the propagation time and c_{ref} is the wave speed in the fuel before the test.

A careful analysis was carried out to establish the influence of the chamber pressurization and the thermal boundary layer in the fuel on the ultrasound measurement. If one uses Eq. (1) for the calculation of the fuel thickness, in typical test conditions, the grain compression is demonstrated to cause errors in measurement whose magnitude is less than 0.3%. On the other hand, the relative error in the thickness measurement caused by the steady-state thermal profile is a function of the grain to the characteristic thermal-layer thickness ratio. This error increases as the thermal boundary layer increases; hence, it decreases as the regression rate increases. To estimate this error, the speed of sound profile in the fuel is required. Measurements of the speed of sound in the polyethylene were carried out in the temperature range of 288–398 K because the melting point of polyethylene is about 410 K, and an exponential form was assumed for the thermal profile.

An analytical expression was developed that predicts that, for instance, with a regression rate of 0.5 mm/s and a thickness of 10 mm the error amounts to 2.5%. For more details see Refs. 10 and 13.

The thickness data were filtered by applying a Gaussian low-pass filter with a cutoff frequency of 3 Hz, then a central formula was applied to take the thickness derivative, that is, for the regression rate calculation.

The time–space averaged regression rate was simply calculated from the equation

$$\bar{\dot{r}} = \bar{\dot{m}}_f / \pi L \rho_f \bar{D} \tag{2}$$

Here, $\bar{D} = (D_0 + \bar{D}_2)/2$ is the time–space average port diameter given by the final fuel mass

$$M_2 = \rho_f L(\pi/4)\left(D_e^2 - \bar{D}_2^2\right) \tag{3}$$

and $\bar{\dot{m}}_f$ is the average fuel mass flow rate that was determined by dividing fuel mass loss by burning duration Δt. Whereas the fuel mass loss is readily measured, establishment of burn time involves the identification of the initial surface regression time and the web burnout time on the pressure–time trace. Here, the inflection point on the primary rise portion of the trace t_0 and the one on the end decrease portion t_2 were assumed, respectively (Fig. 3a). The uncertainty consequent on this method of calculating the average regression rate is estimated to be at most 9.5% (for the minimum burning duration, that is, test 12). In fact, the latter was evaluated taking into account the true initial and final burn instants possibly occurring all along the rising and decreasing parts of the pressure trace, which results in the uncertainties δt_0 and δt_2, respectively. The upper bound of the measurement error is, then, determined conservatively to be nearly equal to $\pm(\delta t_0 + \delta t_2)/2 \cdot \Delta t$ (Fig. 3b).

Incidentally, note that the pressure peaks at $t \cong 2.2$ s and $t \cong 21.2$ s are due to pyrotechnic ignition and nitrogen purge, respectively.

The time–space averaged mass flux is defined based on the average port diameter

$$\bar{G} = 4(\bar{\dot{m}}_f + \bar{\dot{m}}_{ox})/\pi \bar{D}^2 \tag{4}$$

The profiles of the postfiring port diameter were obtained by taking the grain thickness at four circumferential locations with a 45-deg shift and averaging over the measures.

Results and Discussion

Table 1 summarizes the test conditions and the average parameters derived. Time and spatially averaged regression rates are reported in Fig. 4 as a function of the total mass flux together with the data in Refs. 14–16 for comparison. All of the tests in these references were conducted with polyethylene fuel. The first data set from Mitsuno et al.[14] represents the mass flux regression rate results in a ram rocket where the hot combustible gases from the gas generator ignite spontaneously with the air and burn almost completely before they arrive at the entrance of the fuel grain. The second set was obtained from a configuration where the polyethylene fuel was loaded in the gas generator chamber so that, at the same mass flux, the regression rate in this case is several times higher than the one in the former case.

Table 1 Tests table

Test	D_0, mm	p, atm	$\dot{m}_{ox}$, kg/s	Δt, s	$\bar{G}_{ox}$, kg/m^{2}s	$\bar{G}$, kg/m^{2}s	O/F	$\bar{D}$, mm	$\bar{\dot{r}}$, mm/s	x_{max}, mm
1	25	15.63	0.14	24.20	99.69	136.10	2.74	41.71	0.69	280
2	50	16.85	0.13	54.90	27.68	41.21	2.05	75.84	0.47	320
3	16	17.31	0.12	58.30	63.87	89.46	2.50	49.73	0.58	280
4	16	15.64	0.13	43.00	87.14	119.46	2.70	43.48	0.64	——
5	16	15.46	0.12	40.30	92.43	125.90	2.76	41.38	0.63	260
6	25	25.00	0.21	42.60	84.80	113.51	2.95	55.88	0.72	320
7	25	18.96	0.16	50.40	66.60	90.12	2.83	54.73	0.59	——
8	50	22.69	0.19	40.60	47.79	63.96	2.96	70.80	0.51	280
9	75	22.61	0.18	31.50	28.41	39.79	2.50	89.84	0.47	400
10	25	20.25	0.18	21.20	126.00	167.67	3.02	42.33	0.82	320
11	50	20.78	0.17	33.10	47.45	64.85	2.73	68.08	0.55	240
12	75	13.80	0.11	15.20	20.31	31.71	1.78	81.37	0.42	320
13	50	10.09	0.08	26.20	28.19	41.92	2.05	60.04	0.38	320
14	70	15.57	0.12	36.50	20.95	31.03	2.08	84.56	0.40	——
15	75	15.12	0.11	22.80	20.12	30.69	1.90	84.37	0.41	380
16	75	15.48	0.11	25.10	19.93	29.87	2.00	84.72	0.39	280
17	50	12.20	0.10	24.20	34.13	49.75	2.19	60.68	0.44	240
18	16	11.78	0.10	44.10	78.07	107.60	2.64	40.32	0.55	300
19	25	11.11	0.09	44.30	54.03	76.85	2.37	47.19	0.50	No max
20	54	11.96	0.10	50.00	23.00	24.27	2.06	73.04	0.38	260
21	50	9.57	0.08	61.50	18.77	29.46	1.76	71.67	0.35	200

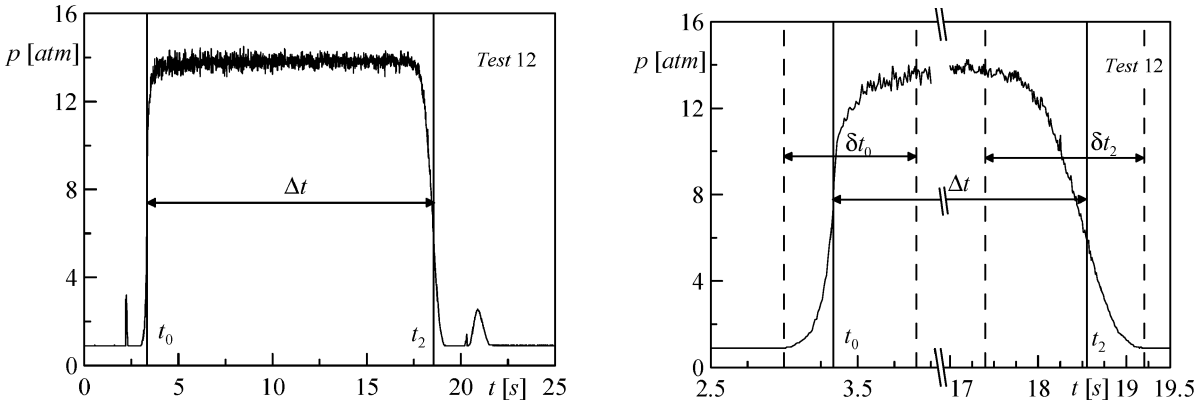

a) Pressure–time trace **b) Initial rise and final decrease of pressure**

Fig. 3 Burn time and its uncertainty definition.

The experimental results of Lengellé et al.[15] come, respectively, from the ONERA planar channel with air preheated at 625 K and from the axisymmetric channel with air heated to high temperatures by means of a precombustion between added oxidizer–fuel flows.

Finally, the series of data from Korting et al.[16] is relative to the combustion of 100% oxygen and polyethylene.

According to Fig. 4, at the same mass flux level and pressure range, the current regression rates display different behavior in terms of both mass flux dependence and magnitude. Whereas it is not possible, in principle, to match up the regression rate magnitude with that of the data from Mitsuno et al. and Lengellé et al. because of the different oxidizer and its initial temperature, some comparisons can be drawn between the regression rate mass flux trends. However, the present results indicate higher regression rates (up to 2.5 times faster than those in the literature) and lower influence of the mass flux itself, as demonstrated by the exponent of the power law. The latter is 0.37 against the values $0.72 \div 1.13$ in the correlations of Mitsuno et al. and Lengellé et al. These exponents are nearly equal to 0.8, which is expected from a fully developed turbulent boundary-layer flowfield. An analogous low mass flux exponent is found by Korting et al.,[16] who also established a pressure dependence, but the reason for this weak influence of mass flux was not clearly explained. Moreover, in the same work, the author performed experiments with a rearward-facing step at the entrance of Plexiglas® grains with a mixture of oxygen and nitrogen as oxidizer. Comparing the regression rates of this case with those expected in similar conditions, when there is no step, Korting et al. found that the latter are considerably lower.

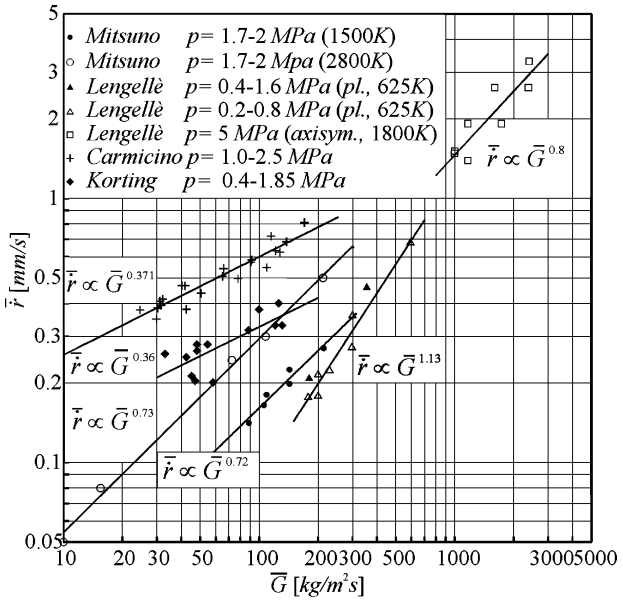

Fig. 4 Comparison of average regression rates.

Oxidizer and its entrance temperature apart, the main difference between the experimental conditions in the works of Mitsuno et al., Lengellé et al., and Korting et al. and those in the present work lies in the way the oxidizer is injected into the port. Indeed, in the first three experimental devices there is no nozzle, but there is an injector chamber that uniformly distributes the oxidizer at the fuel port inlet. This is the cause of the discrepancy in regression behaviors. In fact, in this condition, the oxygen injected by the converging nozzle, generating a flow recirculation zone, leads to a nonuniform convective heat transfer distribution in which the wall heat flux and the regression rate increase from a low value just downstream of the prechamber to a maximum at the jet impingement region and, farther downstream, gradually decrease along the combustor axis. The examination of the port shape after the test reveals fuel consumption profiles coherent with the regression rate distribution described earlier (Fig. 5).

All of the curves in Fig. 5a and 5b, that is, $D_0 = 75$ and 50 mm, respectively, display a maximum whose location, in almost all of the cases, moves downstream as the fuel consumption increases. Different profiles, instead, are shown in Figs. 5c and 5d, that is,

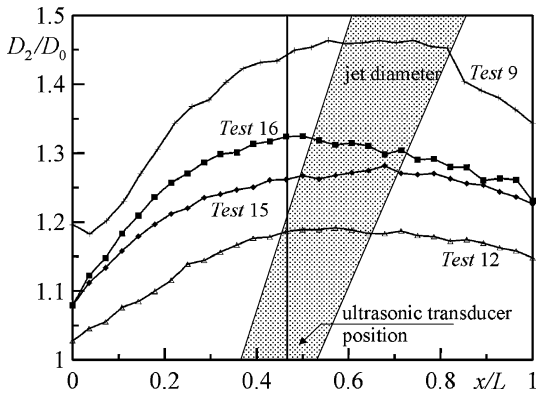

a) $D_0 = 75$ mm

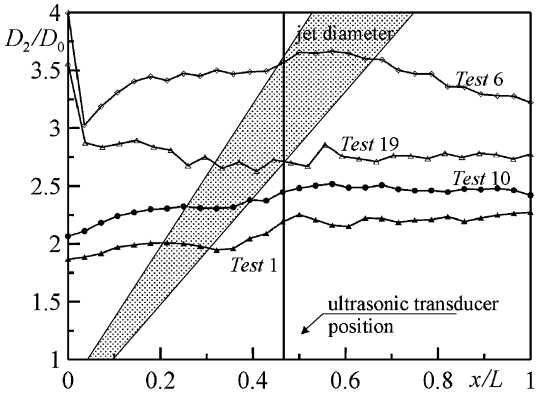

c) $D_0 = 25$ mm

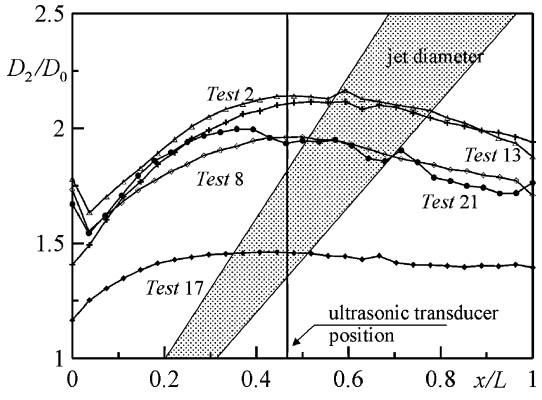

b) $D_0 = 50$ mm

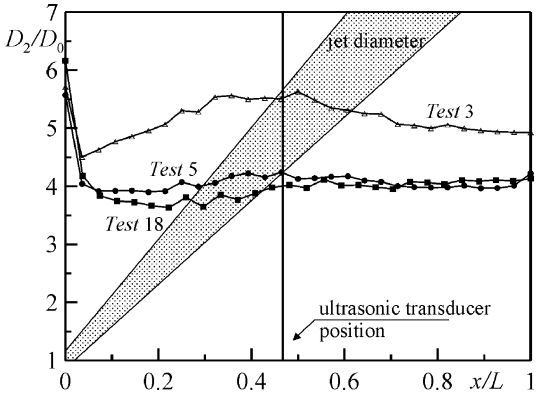

d) $D_0 = 16$ mm

Fig. 5 Afterburn port diameter profiles.

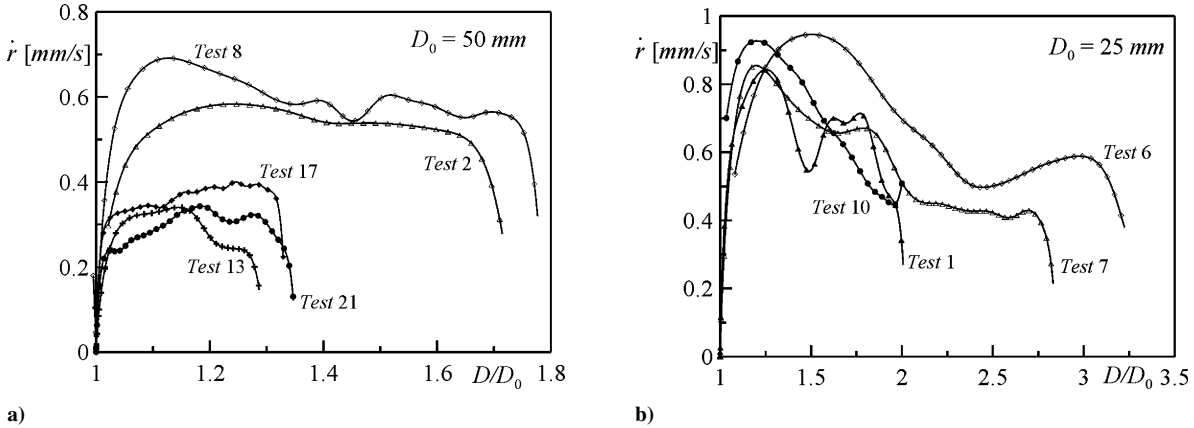

Fig. 6 Local instantaneous regression rates.

$D_0 = 25$ and 16 mm, respectively, by the curves relative to tests 1, 10, and 19 and tests 5 and 18.

Figure 5 also shows the approximate oxidizer jet diameter, which is plotted by assuming a divergence angle varying between 6 and 8 deg according to Ref. 17. Comparison between the jet pattern and the port diameter profiles suggests that the maximum regression rate falls in the region where the oxygen jet impinges on the grain's surface, where the maximum convective heart transfer is expected. For 25- and 16-mm initial diameter grains, this behavior is not so evident, possibly because of the restricted grain length fraction given by the jet impingement. Indeed, also in this case, when larger diameters are reached (or higher fuel consumption is realized), that is, test 6 for $D_0 = 25$ mm and test 3 for $D_0 = 16$ mm, the situation turns quite similar.

A comparison of instantaneous regression rate curves plotted vs the local instantaneous grain diameter (Fig. 6) may support the hypothesis of a strong injection effect. Qualitatively matching the corresponding data in Figs. 5 and 6, one sees that, for $D_0 = 50$ mm, during the run, the oxygen impacts on the grain at the transducer location and so the regression rate appears to be increasing or to be approximately constant. At this point, some remarks have to be made about the curves in Figs. 5 and 6: The final diameter measured by means of the pulse-echo technique did not agree with the one reported in Fig. 6. This can be explained by the fact that the latter is not measured at the transducer position, but is an average value. Thus if the grain's surface is rough, the two measures can be somewhat dissimilar. Furthermore, at the end of the test, when the regression rate goes down, the thermal boundary layer in the grain widens and the speed of sound tends to decrease so that the resulting propagation time is increased. This means that the measured grain thickness is higher than the actual one and the diameter is, in turn, lower.

For example, let us examine in detail the curves of tests 17 and 21. The regression rate meanly increases during the run because the jet impinging region approaches the ultrasonic transducer position. In addition, test 2 represents regression rates first weakly decreasing (after the initial increase due to the startup) until the diameter ratio is equal to about 1.4 (when the jet is roughly under the transducer), and then a change of the regression rate diagram slope occurs. Substantially different behavior occurs for $D_0 = 25$ mm: The regression rate displays a decreasing trend because the region of impingement remains upstream of the transducer except for test 6 in which, actually, the regression rate begins to increase when $D/D_0 \cong 2.4$. Test 7 shows a similar trend, and so, although lacking a postfiring port diameter profile, an analogous situation can be inferred.

This kind of consumption profile is typical of solid fuel ramjets in which a rearward-facing step is placed at the air inlet as the flame stabilizer. In this field of research, Korting et al.,[18] investigating the combustion behavior of polymethylmethacrylate, established regression rate correlations with the mass flux, the exponent of which varied between 0.252 and 0.666, decreasing with pressure levels.

Shulte,[19] who tested polyethylene fuel grains with two internal diameters, found that the average regression rate correlates with the air mass flux in the port and the chamber pressure by $\bar{\dot{r}} \propto p^{0.39}\bar{G}_{\text{air}}^{0.26}$. Gobbo-Ferreira et al.,[20] carrying out an experimental investigation of polyethylene combustion in a solid fuel ramjet, derived the empirical correlation $\bar{\dot{r}} \propto p^{0.8}\bar{G}_{\text{air}}^{0.35}T_{\text{air}}^{0.36}$ valid in the ranges 6.0 atm $< p <$ 11 atm, 300 K $< T_{\text{air}} <$ 787 K, and $\bar{G}_{\text{air}} <$ 16.5 g/cm^{2}s.

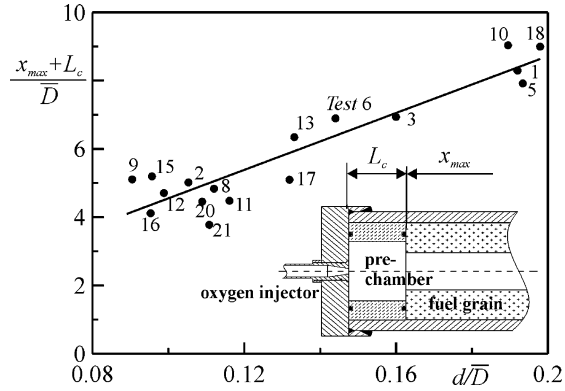

Fig. 7 Maximum regression rate location.

Zvuloni et al.,[21] in a work on the geometric effects on the ramjet combustion with polymethylmethacrylate fuel, found that during an individual extended burning time test at constant mass flow rate, the instantaneous spatially averaged regression rate correlates with the mass flux raised to 0.35. Also, some numerical simulations[22] on the solid fuel ramjet combustor showed a regression rate dependence on mass flux with an exponent equal to 0.3. In conclusion, when the flowfield in the port is dominated by reattachment or impingement regions, as a result the average regression rate is increased and its dependence on mass flux is weakened.

A straight line was used to approximate the location of the maximum fuel consumption (or the recirculation zone length upstream of the jet impingement) as a function of the grain average diameter (Fig. 7):

$$(x_{\max} + L_c)/\bar{D} = 41.7(d/\bar{D}) + 0.384, \qquad R^2 = 0.847 \quad (5)$$

where the sum $x_{\max} + L_c$ is the distance from the injector exit section. This choice may be justified by the assumption that the maximum regression rate coincides with the impingement point on the grain and that the jet spreads linearly, and it is also a usual practice in the analysis of the reattachment zone in solid fuel ramjets.[19,23] Comparing our results with those in the literature does not seem proper, because the latter represent the reattachment length as a function of the step height to the initial diameter ratio. This may be misleading if the burn time is high and $D_2/D_0 \gg 1$, which happens in some present tests when D_2/D_0 reaches values up to 5.5 (Fig. 5). As a matter of fact, $x_{\max}$ in our tests weakly depends on D_0. The relatively large scatter of the data will possibly exist because, in the maximum consumption region, the diameter profile is almost flat and in some cases the grain's surface is wavy.

According to Fig. 7, the point with the maximum deviation from the linear fit, which is about 26%, is the one relative to test 21. The reason can be seen in analyzing the curve (test 21) in Fig. 5b. Here, it is clear that the maximum diameter falls widely upstream of the jet pattern, and this may be responsible for the disagreement in question. However, note that taking into account the average port diameter appears oversimplified because the actual flowfield, as the conduit shape changes, will be somewhat different from that in a pipe.

Correlations Between Regression Rate and Thermofluiddynamic Parameters

For the clear analogy with the flowfield in a solid fuel ramjet, a power correlation was developed to predict the average regression rate as a function of mass flux and pressure. A least-squares fitting procedure yielded

$$\bar{\dot{r}} = 0.0551\bar{G}^{0.362}p^{0.262}, \qquad R^2 = 0.967 \tag{6}$$

In Eq. (6), the regression rate is in millimeters per second, the mass flux in kilograms per square meter seconds, and the pressure in atmospheres. The powers in Eq. (6) are completely comparable with those found in the literature, further demonstrating this analogy.

A deeper understanding of the regression process can be attained by the formulation of an analytical model that starts from the theory developed by Marxman and Gilbert.[1] By considering the convective heat transfer to the surface as the driving force for the fuel regression, they stated that

$$\rho_f \dot{r}/G = 0.023 Re_D^{-0.2} Pr^{-\frac{2}{3}} (St/St_0) B \tag{7}$$

where $St_0 = 0.023 Re_D^{-0.2} Pr^{-2/3}$ is the Stanton number in the turbulent fully developed pipe flows and St is the effective Stanton number for the hybrid rocket with the injection effect.

The Stanton number ratio in Eq. (7) accounts for the reduction in heat flux due to the surface mass addition and can be expressed in terms of the blowing parameter (see Ref. 2). Here, this ratio has to take into account the heat transfer mechanism consequent on the oxidizer injection flow in absence of wall blowing and combustion and, of course, the modified heat transfer for the latter effects.

When this ratio is manipulated, it is possible to assume[10]

$$St/St_0 = (St/St_j)(St_j/St_0) \tag{8}$$

The term St_j/St_0 accounts for the enhanced local heat transfer ensuing from the recirculation zone and the impingement of the jet, whereas the St/St_j ratio explains the additional effects of wall blowing and combustion.

Following Krall and Sparrow,[24] who experimentally investigated the convective heat transfer in the reattachment region of nonreacting flows in circular pipes, one can write

$$St_j/St_0 \approx Nu_{\max}/Nu_0 \propto Re_D^{-0.2}(d/D)^{-\frac{2}{3}} \tag{9}$$

where the first sign does not represent an equality because the correlation has been proven only for the maximum heat transfer Nusselt number $Nu_{\max}$.

Rearranging Eq. (7) and referring to the average parameters yields

$$\rho_f \bar{\dot{r}}/\bar{G} = 0.023\, Pr^{-\frac{2}{3}} Re_{\bar{D}}^{-0.4}(d/\bar{D})^{-\frac{2}{3}}(\overline{St}/\overline{St_j})\bar{B} \tag{10}$$

Two comments have to be made: First, Eq. (10) predicts that the regression rate depends on mass flux with a power of 0.6, that is, less than that for a fully developed flow; second, port diameter explicitly influences regression rate.

If the variation of the last two terms in Eg. (10) is ignored, a correlation of regression rate with mass flux and average diameter is obtained:

$$\bar{\dot{r}} = 0.00349\, \bar{G}^{0.642}\bar{D}^{0.568}, \qquad R^2 = 0.973 \tag{11}$$

Here, the average diameter is in millimeters. In this correlation the exponent of the Reynolds number and that of the diameters ratio were released to permit a dependence of the average values different from that in Eq. (10).

Therefore, in these instances, it is not possible to ascertain if there is a real pressure effect or if it is just a geometrical effect influencing the regression rate. Although Eq. (11) represents a useful and easy to manage engineering correlation, it neglects the influence of the blowing parameter variation on regression rate and lumps it in the pre-constant. To achieve a more realistic and possibly accurate correlation, the blowing parameter B was calculated using the relationship

$$B = (h_f - h_w)/H_v \tag{12}$$

where $h_f - h_w$ is the enthalpy difference between the flame and the wall. The calculation of both terms contained in Eq. (12) involves the knowledge of surface temperature. The latter was estimated by using an Arrhenius law for the solid fuel regression rate as a function of surface temperature itself, namely,

$$\bar{\dot{r}} = A \exp(-E_a/2R_g T_w) \tag{13}$$

where, from Ref. 15, the activation energy $E_a = 60$ kcal/mole and the preexponential factor $A = 4.78 \times 10^6$ mm/s. Note that this technique for correlating surface temperature and regression rate is quite customary,[3,4,25] and it does not imply that the chemical reaction rate of the fuel decomposition decides the regression rate. Rather, it must be recognized as complementary to the heat transfer approach [Eq. (7)] to solve for the unknown surface temperature. In fact, because of the relatively large activation energy for depolymerization, an increase in heat transfer will produce a corresponding increase in the regression rate with very little change in the surface temperature and, in contrast, a very large variation in the regression rate can be accomplished with a relatively small temperature adjustment. In this situation, a simple proportionality between the surface heat flux and the regression rate, as stated in Eq. (7), is possible. Thus, such a process is definitely controlled by the heat flux to the fuel surface, and reaction kinetics only play a minor role.[1] Under the assumption that the pyrolyzed gas at the surface is composed of only the ethylene monomer, the blowing number was computed with a chemical equilibrium code,[26] calculating the effective heat of vaporization as reported in Ref. 27.

The Stanton number was then calculated from Eq. (7):

$$\overline{St} = [(\rho_f \bar{\dot{r}})/\bar{G}](1/\bar{B}) \tag{14}$$

An expression of the Stanton number as a power of the Reynolds number, the injector to average port diameter ratio and the blowing number was searched for by allowing the exponents to vary to best fit the experimental data. The result of this analysis yielded

$$\rho_f \bar{\dot{r}}/\bar{G} = 0.716 Re_{\bar{D}}^{-0.596}(d/\bar{D})^{-0.850}\bar{B}^{-0.160}, \qquad R^2 = 0.981 \tag{15}$$

First, note that by considering the influence of B, the experimental data are best correlated with mass flux and average port diameter powers different from those in Eq. (11), and this demonstrates that the blowing number has a nonnegligible role. Furthermore, the correlation factor is higher than the one relative to Eq. (11), and this implies somewhat improved accuracy; in particular, the error band amplitude is $\pm 10\%$ (Fig. 8), which reasonably coincides with the regression rate measurement uncertainty.

Second, the powers of both the Reynolds number and the diameter ratio are almost different from those in Eq. (10) as well, indicating that the heat transfer distribution in the hybrid rocket studied here is not accurately described by imposing the correlation developed by Krall and Sparrow, that is, Eq. (9). Indeed, the concave profile of the port (Fig. 5) certainly modifies the flow with respect to that in conventional circular pipes. In a previous work, assuming that (St/St_j) depends on the blowing number and expressing the latter as a function of the oxidizer to fuel ratio, Carmicino and Russo Sorge[10] attempted to correlate the same experimental data with Eq. (10), letting the parameters in this function vary. The result was a nondimensional relationship with practically the same correlation factor. However, here it is believed that this operation might

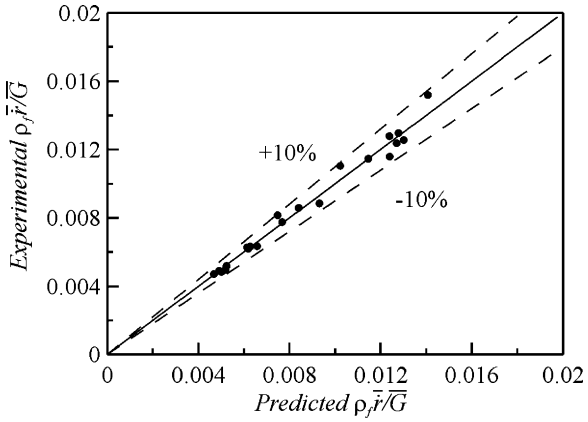

Fig. 8 Semi-empirical regression rate correlation result.

be misleading because, based on just a statistical analysis, though it correlates the data well, it leads to a dependence of the blowing number on the mixture ratio that is not real.

Conclusions

This work aimed to investigate the regression rate characteristics in a hybrid rocket where the oxidizer is injected through a conical axial nozzle rather than a stagnation chamber. Time–space averaged regression rates measured in this study, by comparison with some data in the literature, at the same oxidizer mass flux and chamber pressure, exhibited weaker mass flux dependence. The concave port diameter profiles, with a region of maximum fuel consumption, indicated that nonuniform oxygen injection must strongly influence the heat transfer mechanism that resembles the one in solid fuel ramjets with a rearward-facing step at the air inlet, rather than the one typical of fully developed pipe flow. This feature leads to the verified lower dependence of regression rate on mass flux and introduces a pure geometric effect that is an explicit regression rate dependence on the grain diameter. The ultrasounds pulse-echo technique was further used to gather more information on the local regression rate behavior during the run. The local instantaneous regression rates showed that, in some instances, depending on the relative position of the oxygen impingement zone on the grain's surface and the ultrasonic transducer location, the burn rate is constant or increases during the run. In fact, this behavior can be explained by considering the oxidizer impinging jet zone dynamics.

Effects produced by the injection in classical hybrids are often underestimated. They have been demonstrated here to be of primary importance and worthy of further in-depth study.

A nondimensional correlation involving the Reynolds number, the injector to grain diameter ratio, and the blowing number was developed with good accuracy of the predicted data. In any case, care has to be taken in the extrapolation of the results provided by this correlation to other rocket configurations. In particular, it ignores the effect of grain length to diameter ratio, which certainly plays a fundamental role in the definition of the powers. The injection effect, indeed, is expected to be more important when the extent of the impinging region is larger compared to the grain length.

Acknowledgments

This work, as with the entire research activity of the University of Naples "Federico II" in the aerospace propulsion field, has been carried out thanks to the hospitality of the Italian Military Air Force, which has given us an area in the Francesco Baracca Airport (Grazzanise, Caserta) where the Propulsion Laboratory was built. ASI and MURST sponsored the work. The authors wish to thank all of the graduating students who contributed to the experimental apparatus setup and to the development of tests campaign.

References

[1]Marxman, G. A., and Gilbert, M., "Turbulent Boundary Layer Combustion in the Hybrid Rocket," *Ninth International Symposium on Combustion*, Academic Press, New York, 1963, pp. 371–383.

[2]Marxman, G. A., "Combustion in the Turbulent Boundary Layer on a Vaporizing Surface," *Tenth International Symposium on Combustion*, Combustion Inst., Pittsburgh, PA, 1965, pp. 1337–1349.

[3]Chiaverini, M. J., Serin, N., Johnson, D. K., Lu, Y., Kuo, K. K., and Risha G. A., "Regression Rate Behavior of Hybrid Rocket Solid Fuel," *Journal of Propulsion and Power*, Vol. 16, No. 1, 2000, pp. 125–132.

[4]Chiaverini, M. J., Kuo, K. K., Peretz, A., and Harting, G. C., "Regression Rate and Heat Transfer Correlations for Hybrid Rocket Combustion," *Journal of Propulsion and Power*, Vol. 17, No. 1, 2001, pp. 99–110.

[5]Smoot, L. D., and Price, C. F., "Pressure Dependence of Hybrid Fuel Regression Rates," *AIAA Journal*, Vol. 5, No. 1, 1967, pp. 102–106.

[6]Wooldridge, C. E., Marxman, G. A., and Kier, R. J., "Investigation of Combustion Instability in Hybrid Rockets," NASA Contract NAS 1-7310, Stanford Research Inst., Stanford Univ., Stanford, CA, 1969.

[7]Altman, D., and Humble, R., "Hybrid Rocket Propulsion Systems," *Space Propulsion Analysis and Design*, 1st ed., rev., McGraw–Hill, New York, 1995, pp. 392–401.

[8]Muzzy, R. J., "Applied Hybrid Combustion Theory," AIAA Paper 72-1143, Nov. 1972.

[9]Carmicino, C., Giulietti, G., Marchione, T., Lavorgna, F., and Russo Sorge, A., "Regression Rate Measurements in a Hybrid Rocket," *Proceedings of the 8th International Workshop on Combustion and Propulsion*, Grafiche g.s.s., Bergamo, Italy, 2002, pp. 13-1–13-10.

[10]Carmicino, C., and Russo Sorge, A., "Investigation of the Fuel Regression Rate Dependence on Oxidizer Injection and Chamber Pressure in a Hybrid Rocket," AIAA Paper 2003-4591, July 2003.

[11]Russo Sorge, A., "The State of Art of Hybrid Propulsion Research in Italy," *Proceedings of the 8th International Workshop on Combustion and Propulsion*, Grafiche g.s.s., Bergamo, Italy, 2002, pp. 09-1–09-7.

[12]Traineau, J. C., and Kuentzmann, P., "Ultrasonic Measurements of Solid Propellant Burning Rates in Nozzleless Rocket Motors," *Journal of Propulsion and Power*, Vol. 2, No. 3, 1986, pp. 215–222.

[13]Carmicino, C., "Alcuni aspetti della balistica interna di un endoreattore a propellenti ibridi e del comportamento di ugelli a spina troncata," Tesi di Dottorato di Ricerca, Univ. degli Studi di Napoli "Federico II," Naples, Italy, Nov. 2002.

[14]Mitsuno, M., Kuwabara, T., Kosaka, K., and Shirota, K., "Experimental Study on Solid Fuel Ram Rocket," International Aeronautical Federation, IAF80 F269, Sept. 1980.

[15]Lengellé, G., Fourest, B., Godon, J. C., and Guin, C., "Condensed Phase Behavior and Ablation Rate of Fuels for Hybrid Propulsion," AIAA Paper 93-2413, June 1993.

[16]Korting, P. A. O. G., Schöyer, H. F. R., and Timnat, Y. M., "Advanced Hybrid Rocket Motor Experiments," *Acta Astronautica*, Vol. 15, No. 2, 1987, pp. 97–104.

[17]Abramovich, G. N., "The Theory of Turbulent Jets," Massachussets Inst. of Technology Press, Cambridge, MA, Sept. 1963, pp. 3–17.

[18]Korting, P. A. O. G., Van der Geld, C. W. M., Wijchers, T., and Schöyer, H. F. R., "Combustion of Polymethylmethacrylate in a Solid Fuel Ramjet," *Journal of Propulsion and Power*, Vol. 6, No. 3, 1990, pp. 263–270.

[19]Shulte, G., "Fuel Regression and Flame Stabilization Studies of Solid-Fuel Ramjets," *Journal of Propulsion and Power*, Vol. 2, No. 4, 1986, pp. 301–304.

[20]Gobbo-Ferreira, J., Silva, M. G., and Carvalho, J. R., "Performance of an Experimental Polyethylene Solid Fuel Ramjet," *Acta Astronautica*, Vol. 45, No. 1, 1999, pp. 11–18.

[21]Zvuloni, R., Gany, A., and Levy, Y., "Geometric Effects on the Combustion in Solid Fuel Ramjets," *Journal of Propulsion and Power*, Vol. 5, No. 1, 1989, pp. 32–37.

[22]Netzer, D. W., "Modeling Solid Fuel Ramjet Combustion," *Journal of Spacecraft and Rockets*, Vol. 14, No. 12, 1977, pp. 762–766.

[23]Krishnan, S., and George, P., "Solid Fuel Ramjet Combustor Design," *Progress in Aerospace Sciences*, Vol. 34, Nos. 3–4, 1998, pp. 219–256.

[24]Krall, K. M., and Sparrow, E. M., "Turbulent Heat Transfer in the Separated, Reattached, and Redevelopment Regions of a Circular Tube," *Journal of Heat Transfer*, Vol. 8, Feb. 1966, pp. 131–136.

[25]Knuth, W. H., Chiaverini, M. J., Sauer, J. A., and Gramer, D. J., "Solid-Fuel Regression Rate Behavior of Vortex Hybrid Rocket Engines," *Journal of Propulsion and Power*, Vol. 18, No. 3, 2002, pp. 600–609.

[26]Gordon, S., and McBride, B. J., "Computer Program of Complex Chemical Equilibrium Compositions and Applications," NASA Reference Publ. 1311, Oct. 1994.

[27]de Wilde, J. P., "The Heat of Gasification of Polyethylene and Polymethylmethacrilate," Rept. PML 1988-C42, ŠFCC Publ. 53, Faculty of Aerospace Engineering/Prins Maurits Lab./Solid Fuel Combustion Chamber, Delft Univ. of Technology, Delft, The Netherlands, Sept. 1988.